Talanta 262 (2023) 124723

Contents lists available at ScienceDirect

Talanta

journal homepage: www.elsevier.com/locate/talanta

Domino protocol for the synthesis of diversely functionalized derivatives of a novel fused pentacyclic antioxidant/anticancer fluorescent scaffold: Pyrazolo[5'',1'':2',3']pyrimido[4',5':5,6][1,4]thiazino[2,3-b]quinoxaline

Seddigheh Sheikhi-Mohammareh [a], Fatemeh Oroojalian [b,c], Hamid Beyzaei [d], Mohammadreza Moghaddam-Manesh [e], Alireza Salimi [a], Fatemeh Azizollahi [b], Ali Shiri [a,*]

[a] Department of Chemistry, Faculty of Science, Ferdowsi University of Mashhad, Mashhad, Iran
[b] Department of Advanced Sciences and Technologies, School of Medicine, North Khorasan University of Medical Sciences, Bojnurd, Iran
[c] Natural Products and Medicinal Plants Research Center, North Khorasan University of Medical Sciences, Bojnurd, Iran
[d] Department of Chemistry, Faculty of Science, University of Zabol, Zabol, Iran
[e] General Bureau of Standard Sistan and Baluchestan Province, Iranian National Standards Organization, Zahedan, Iran

ARTICLE INFO

Handling Editor: J. Wang

Keywords:
One-pot
Quinoxaline
Fluorescent
Antioxidant
Anticancer
Pyrazolo[1,5-*a*]pyrimidine
pyrazolo[5″,1'':2′,3']pyrimido[4′,5':5,6][1,4]thiazino[2,3-*b*]quinoxaline

ABSTRACT

Rising to the challenge of formidable multi-step reaction needed for the synthesis of polycyclic compounds, an efficient one-pot two-step procedure for the synthesis of densely functionalized novel pyrazolo[5″,1'':2′,3'] pyrimido[4′,5':5,6] [1,4]thiazino[2,3-*b*]quinoxalines from synthetically accessible starting materials 6-bromo-7-chloro-3-cyano-2-(ethylthio)-5-methylpyrazolo[1,5-*a*]pyrimidine, 3-aminoquinoxaline-2-thiol and some readily accessible alkyl halides was established. The domino reaction pathway involves cyclocondensation/*N*-alkylation sequence in K_2CO_3/*N,N*-dimethyl formamide under heating condition. DPPH free radical scavenging activity of all synthesized pyrazolo[5″,1'':2′,3']pyrimido[4′,5':5,6][1,4]thiazino[2,3-*b*]quinoxalines was evaluated to determine their antioxidant potentials. IC_{50} values were recorded in the range of 29–71 μM. *N*-benzyl substituted derivative represented the most effective antioxidant activity as well as antiproliferative activity against MCF-7 cells. Moreover, fluorescence in solution for these compounds exhibited strong red emission in the visible region ($\lambda_{flu.}$ = 536–558 nm) with good to excellent quantum yields (61–95%). Due to their interesting fluorescence properties, these novel pentacyclic fluorophores can be used as fluorescent markers and probes for studies in biochemistry and pharmacology.

1. Introduction

During the last decades, studies on the synthesis and chemistry of new quinoxalines have attracted considerable attention because of their interesting chemical as well as biological properties. Quinoxalines have anti-viral [1], anti-bacterial [2], anti-inflammatory [3], anti-protozoal [4], anti-cancer [5], anti-depressant [6], anti-HIV activities [7] and are also kinase inhibitors [8]. Furthermore, quinoxaline units are present in the structure of various antibiotics such as echinomycin, levomycin and actinoleutin, which are known to inhibit the growth of Gram-positive bacteria and are active against various transplantable tumors [9,10]. In addition, quinoxaline derivatives are used in dyes [11], efficient electron luminescent materials [12], organic semiconductors [13], chemically controllable switches [14], building blocks for the synthesis of anion receptors [15], cavitands [16] and dehydroannulenes [17]. They also serve as useful rigid subunits in macrocyclic receptors in molecular recognition [18]. Some quinoxaline derivatives have been synthesized using microwave irradiation [19]. However, recent synthetic methods have focused on techniques involving alternative activation modes like the condensation of 1,2-diamines with α-diketones [20], 1,4-addition of 1,2-diamines [21] to diazenylbutenes [22], cyclisation–oxidation of phenacyl bromides and oxidative coupling of epoxides with ene-1,2-diamines [23–25].

On the other hand, the synthesis of pyrazolo[1,5-*a*]pyrimidine derivatives and the investigation of their chemical and biological behavior has attracted a great deal of attention due to pharmaceutical reasons [26,27]. For example, the hypnotic drug Zaleplon **(I)**, the anticancer agent Dinaciclib **(II)**, the fungicide Pyrazophos **(III)** have the structural

* Corresponding author.
E-mail address: alishiri@um.ac.ir (A. Shiri).

https://doi.org/10.1016/j.talanta.2023.124723
Received 9 February 2023; Received in revised form 4 May 2023; Accepted 22 May 2023
Available online 24 May 2023

motif of pyrazolo[1,5-*a*]pyrimidine [28–31]. (Fig. 1).

Because of the importance of pyrazolo[1,5-*a*]pyrimidine scaffold, various methods for its synthesis has been developed. Most of them involve the condensation reaction between aminopyrazoles and 1,3-*bis*-electrophilic reagents, such as 1,2-allenic ketones [32], enaminones [33], enaminonitriles [26], β-ketonitriles [34], 1,3-dicarbonyl compounds [35] and α,β unsaturated carbonyl compounds [36].

Therefore, in continuation to our ongoing endeavor toward developing novel pharmacologically significant heterocyclic architectures [35,37–44] and with the perspective on opening an avenue to imaging studies of cells and tissues in biochemistry and pharmacology, we wish to reveal the detailed antioxidant, antiproliferative as well as fluorescent properties of derivatives of pyrazolo[5″,1'':2′,3']pyrimido[4′,5':5,6][1,4]thiazino[2,3-*b*]quinoxaline as a novel heterocyclic system **(4a-e)** which were synthesized via tandem reaction of 3-aminoquinoxaline-2-thiol (**1**) with pyrazolo[1,5-*a*]pyrimidine (**2**) followed by *N*-alkylation in K_2CO_3/DMF.

2. Results and discussion

2.1. Chemistry

To trigger our project, 3-aminoquinoxaline-2-thiol **(1)** and 6-bromo-7-chloro-3-cyano-2-(ethylthio)-5-methyl-pyrazolo[1,5-*a*]pyrimidine **(2)** as starting materials were synthetically prepared according to previously reported procedures [20,35]. Subsequently, employing a one-pot two-step sequential procedure involving hetero-annulation/*N*-alkylation between compound **(1)** and 6-Bromo-7-chloro-3-cyano-2-(ethylthio)-5-methylpyrazolo[1,5-*a*]pyrimidine **(2)** in the presence of several alkyl halides in K_2CO_3/DMF at 80–90 °C was led to form various novel highly functionalized pyrazolo[5″,1'':2′,3']pyrimido[4′,5':5,6][1,4]thiazino[2,3-*b*]quinoxalines **(4a-e)** through the fused five cyclic intermediate **(3)**. (Scheme 1).

The structural assignment of adduct **(3)** is based upon spectroscopic and micro-analytical data. The ^{1}H NMR spectrum of it shows the signals of ethyl moiety at δ 1.29 ppm and δ 3.17 ppm. The methyl group is assigned as singlet at δ 2.00 and aromatic protons as multiple signals around δ 7.01–7.37 ppm. The signal of NH is missing in the spectrum. The IR spectrum of **(3)** shows the stretching vibration bands of CN and NH groups at 2213 cm^{-1} and 3347 cm^{-1}, respectively. Additionally, the observation of molecular ion peak at *m/z* 391 in the mass spectrum as well as the mass of $[M+H]^+$: 392.0752 in HRMS confirms the occurrence of a heterocycle with $C_{18}H_{14}N_7S_2$ formula.

Moreover, compound **(4a)** as an alkylated derivative shows two singlet peaks at δ 2.45 and 3.96 ppm belonging to methyl groups of the pyrimidine and thiazine moieties in ^{1}H NMR spectrum, respectively. The thioethyl ether signals are observed at δ 1.38 (triplet) and δ 3.25 ppm (quartet). Also, the spectrum shows a multiple signal in the region of δ 7.51–7.71 ppm corresponding to the aromatic protons. The HRMS test of **(4a)** shows the molecular ion peak of $[M+H]^+$ at 406.0903 which corroborate the molecular formula of $C_{19}H_{16}N_7S_2$.

2.2. PXRD analysis of compound (4a)

Despite our best endeavors, we could not obtain a suitable single crystal for the work to be unambiguous through the dissolving of each of the newly synthesized compounds in different situations as in solvent, methods, or temperature conditions during months. In this regard, PXRD analysis of compound **(4a)** was established as an additional evaluation to investigate the framework of our products. The powder XRD pattern was indexed at a low angle using the program DICVOL04 [45], to give a monoclinic system and approximate cell parameters of a = 19.3442 Å, b = 15.4175 Å, c = 8.3154 Å and β = 95.3613° with the good figure of merits [M (12) = 14.9; F (12) = 34.8(0.0172, 20)]. The unit cell and profile refinements were carried out using Rietveld method [46,47] which led to a good fit and obtain a good R-factor of the whole profile with Rwp = 8.31%, R_p = 12.8%, $\chi^2 = 0.37$. The Rietveld refinement was performed with the aid of the Full Prof suite of programs [48]. The experimental, calculated (according to best-fit parameters), and difference patterns are shown in Fig. 2. The results showed that there is a good agreement between experimental and calculated data.

According to single X-ray crystallography analysis in our previous study [35] in which the true regio-isomer has been established and due to the structural similarity of binucleophiles (ortho amino thiophenol in previous work & 3-aminoquinoxaline-2-thiol in the present work) (Scheme 2), it can be rationalized that heterocyclization of compounds **(3 & 4a-e)** most likely proceeded through two successive S_NAr mechanisms by nucleophilic attack of adjacent NH_2 and SH groups of nucleophile **(1)** on vicinal chlorine and bromine of pyrazolopyrimidine **(2)**, respectively. Additionally, the comparison of cell parameters between previously reported structure [35] (a = 7.9902(4)Å, b = 13.9443(7)Å c = 13.8171(7)Å, and β = 90.4370(7)°) and compound **(4a)** indicated that these structures have the same crystal system.

2.3. Photophysical study

Fluorescent probes with large Stokes shifts, high quantum yields and red/near-infrared emission are effective tools for the biomedical research. They include biomolecule labels, medical diagnostic imaging, high-resolution imaging-navigated surgery, and enzyme assays [49–54]. However, these traditional probes (dyes) such as fluorescein, rhodamine, and cyanine usually display small Stokes shifts (less than 30 nm) or low quantum yields [55,56]. According to the literatures, introducing tetrahydro quinoxaline unit on fluorophore is a feasible method to regulate Stokes shifts or improving quantum yields [57].

The goal of this project was to develop a straightforward approach to the synthesis of various derivatives of pyrazolo[5″,1'':2′,3']pyrimido[4′,5':5,6][1,4]thiazino[2,3-*b*]quinoxaline as a novel heterocyclic system and further polarization of the whole system in pyrazolo-pyrimido-thiazino-quinoxaline derivatives **(3 & 4a-e)**, through improved push-pull effect by placing a –CN moiety (electron withdrawing group) at the opposite side of the planar heterocycle from a tertiary amino group (electron donating group) leading to desirable optical response.

To probe the photophysical attributes of the fused pentacyclic frameworks of **(3 & 4a-e)**, the UV and fluorescence spectroscopy was

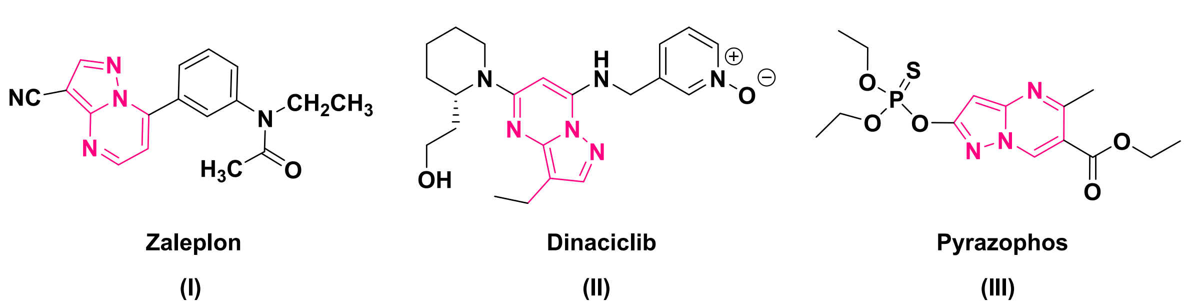

Fig. 1. Examples of pharmacologically active pyrazolo[1,5-*a*]pyrimidines.

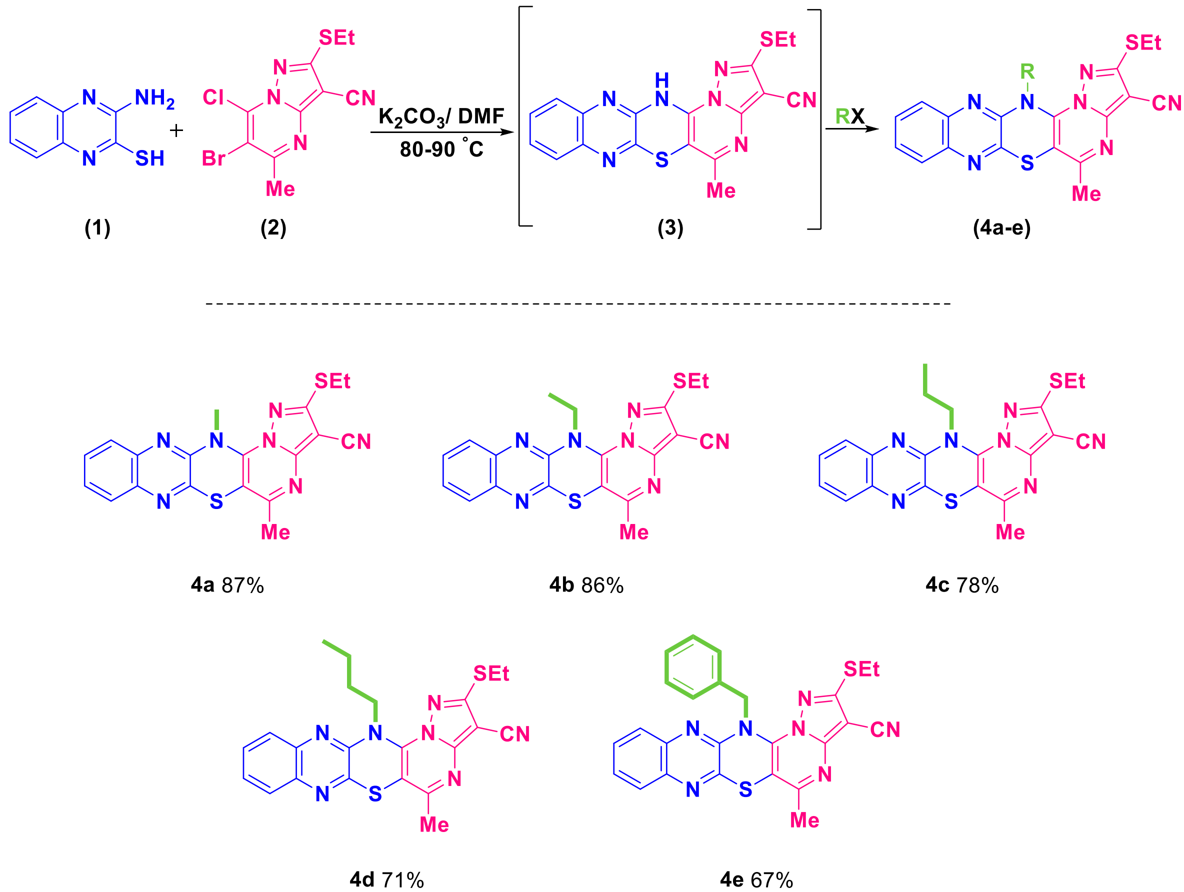

Scheme 1. Synthesis pathway to pyrazolo[5″,1'':2′,3']pyrimido[4′,5':5,6][1,4]thiazino[2,3-*b*]quinoxalines.

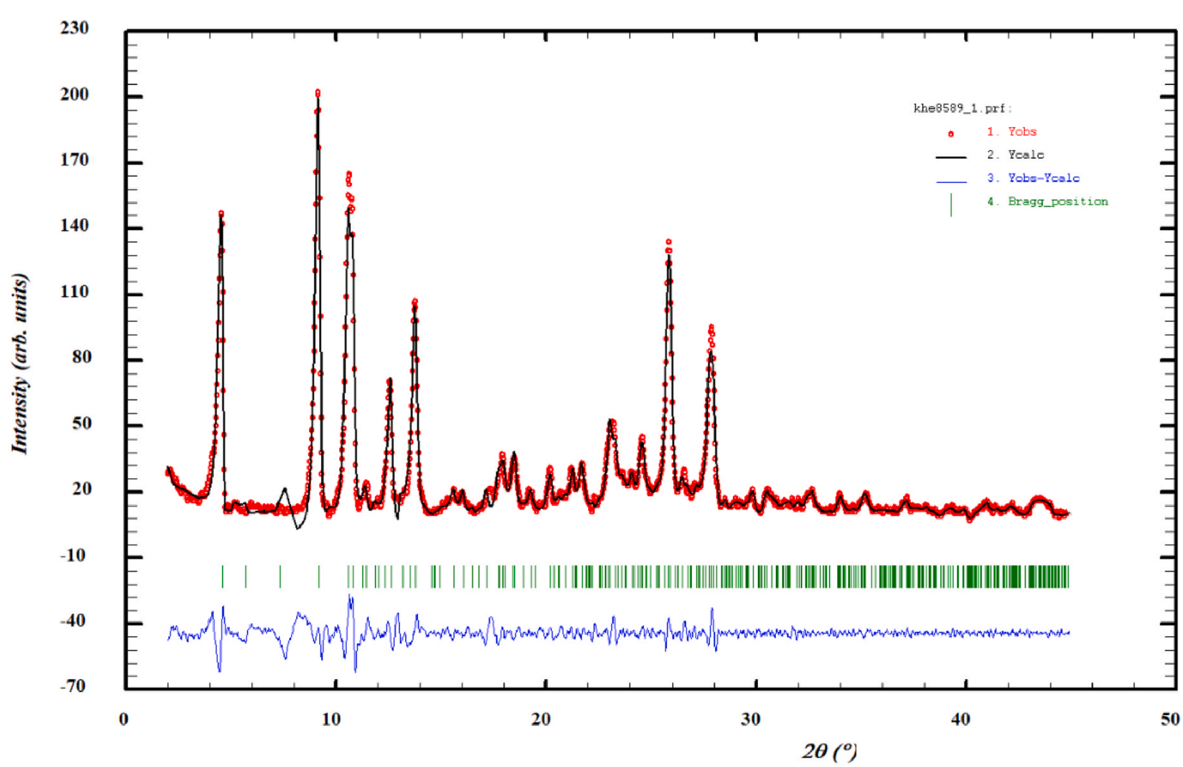

Fig. 2. Rietveld refinement of **(4a)**, showing the experimental (+), calculated (−) and difference (bottom) powder X-ray diffraction profiles. Reflection positions are marked.

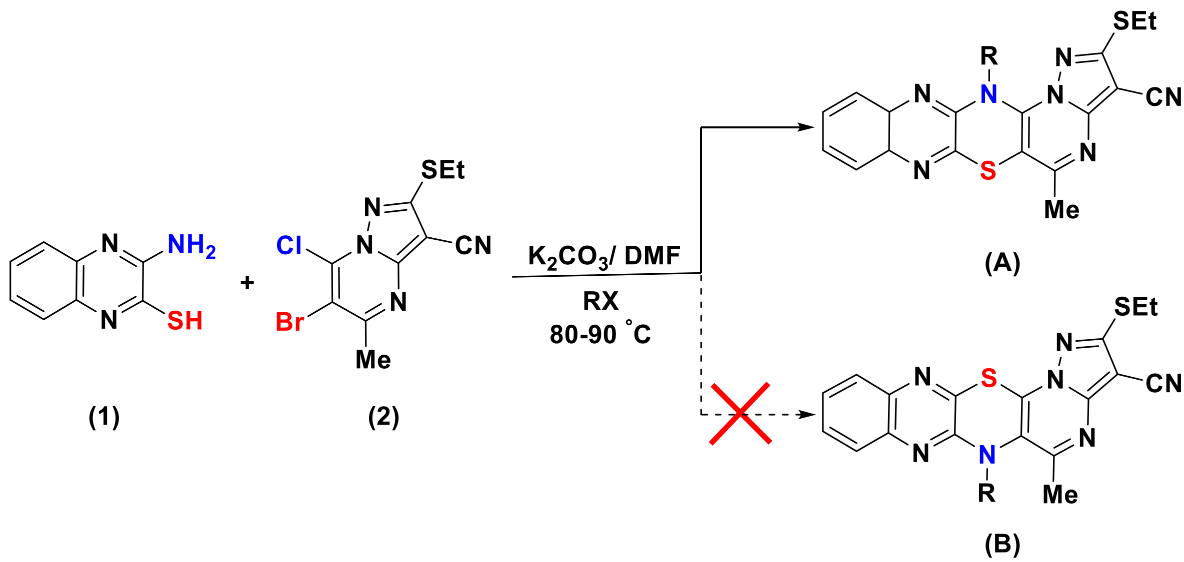

Scheme 2. Regio isomeric possibilities for one-pot heterocyclization of derivatives.

adopted in the wavelength range of 250–800 nm. The spectral data of compounds **(3 & 4a-e)** such as wavelengths of maximum absorbance (λ_{abs}[nm]), extinction coefficients ($\varepsilon \times 10^4$[M^{-1}. cm^{-1}]), wavelengths of fluorescence excitation (λ_{ex}[nm]), wavelengths of fluorescence emission (λ_{flu}[nm]), fluorescence quantum yields (Φ_F), and Stokes shift [nm] are summarized in Table 1. The values of extinction coefficient (ε) are calculated as the slope of the plot of absorbance *vs* concentration.

Because of the high solubility of the compound **(4b)** in DMF, it was selected as a model solvent and the absorption spectrum of **(4b)** was scanned in DMF (2×10^{-5} M). (Fig. 3).

The maximum absorption wavelengths (λ_{max}) were observed in 471, 501 and 536 nm (in the visible region) but the highest emission was detected when the compound was excited at λ = 471 nm. These absorption bands probably belong to π–π* transitions. The position of the absorption bond remained almost constant with different lengths of the alkyl chain in compounds **(4a-e)**. Compared with the average, the absorption peak wavelength for **(3)** was red-shifted by 3.5 nm. This bathochromic phenomenon could spring from an electronic effect, which lowers the HOMO-LUMO band gap due to the presence of a strong mesomeric effect (a fully extended conjugation) from NH moiety (EDG) to –CN group (EWG) as well as an elongated H-migration length on the other nitrogens of the main heterocyclic architecture. The opposite of this effect occurs in the fluorescence spectrum of compound 3 (blue-shift to $\lambda_{flu.}$ = 536 nm in comparison to other fluorescence wavelengths). Therefore, the least stokes shift (60 nm) belongs to it.

Emission spectrum of compounds **(3 & 4a-e)** at $\lambda_{ex.}$ 471–476 nm in dilute DMF solution (2×10^{-6} M) is depicted in Fig. 4. The fluorescence quantum yield (Φ_F) which is the ratio of photons absorbed to photons emitted through fluorescence relative to fluorescein as the reference compound were calculated according to the literature [58]. The Φ_F of compounds **(3 & 4a-e)** amounts to the range of 0.61–0.95, which may be compared to the quantum yield of fluorescein as the well-known fluorescent dye (Φ_F = 0.95). These highly fluorescent compounds **(3 & 4a-e)** exhibited significantly higher quantum yields than those for similar

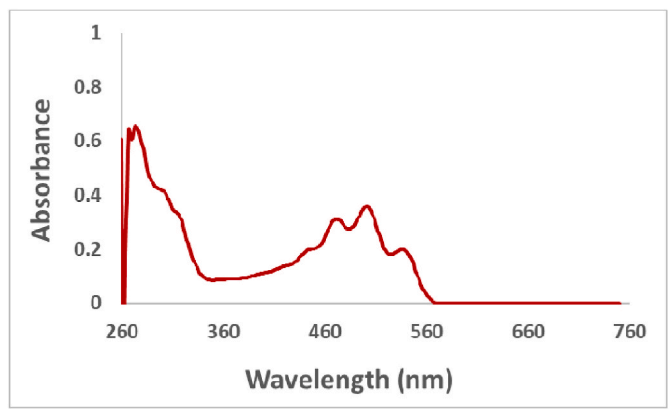

Fig. 3. UV/Vis absorption spectrum of compound **(4b)** in DMF solution (2×10^{-5} M).

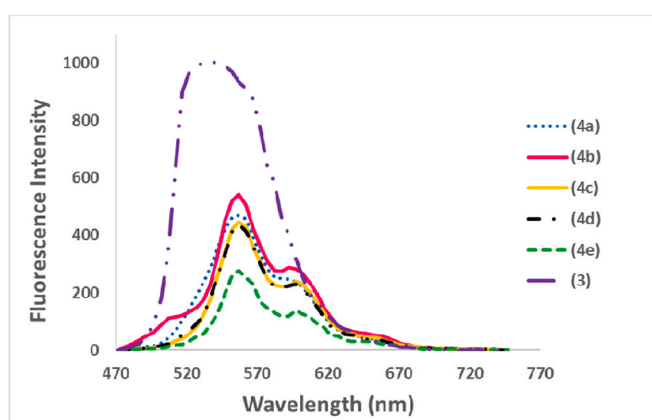

Fig. 4. Emission spectrum of compounds **(3 & 4a-e)** at $\lambda_{ex.}$ 471–476 nm in dilute DMF solution (2×10^{-6} M).

Table 1
Photophysical properties of (3 & 4a-e) in DMF.

Dye	$\lambda_{abs.}$ (nm)	$\epsilon \times 10^4$ ($M^{-1}cm^{-1}$)[a]	$\lambda_{ex.}$ (nm)	$\lambda_{flu.}$ (nm)	Φ_F [b]	Stokes shift (nm)
(3)	476	0.73	476	536	0.95	60
(4a)	472	1.64	472	557	0.74	85
(4b)	471	1.22	471	556	0.79	85
(4c)	471	1.51	471	556	0.72	85
(4d)	472	1.57	472	557	0.72	85
(4e)	473	1.41	473	558	0.61	85

[a] Extinction coefficient.
[b] Quantum yield of fluorescein in MeOH as standard is Φ_F = 0.95.

benzothiadiazoles (Φ_F = 0.19–0.20) [59] and quinoxalines (Φ_F = 0.54–0.62) [60]. When a hetero nitrogen is singly bonded to carbon atoms in a heterocycle, as in thiazine ring, the transitions involve the non-bonding electrons resembling to those of π–π* transitions. In fact, the non-bonding orbital is perpendicular to the plane of the ring, which allows it to overlap the p orbitals on the adjacent carbon atoms. The relatively high fluorescence quantum yield of the newly synthesized compounds **(4a-e)** can be explained in the same way due to the intramolecular charge transfer (ICT) states [61] from the donor site (endocyclic N) to the acceptor moiety (-CN group). The self-explanatory and plausible push-pull mechanism of donor-π-acceptor (D-π-A) heterocyclic dyes **(4a-e)** with an endocyclic tertiary amino group as a strong donor, pyrazolopyrimidine heterocyclic scaffold as a planar π-spacer and –CN group as a strong acceptor is depicted in Scheme 3.

Compound **(3)** with vastly superior fluorescence intensity and emission quantum yield (Φ_F = 0.95) among the other dyes **(4a-e)** was recognized as a supreme florescent heterocyclic compound. Surprisingly enough, compound **(3)** with the same Φ_F value as fluorescein can be introduced as a promising fluorescent dye.

2.3.1. Solvatofluorochromism effects

In general, the emission spectra of chemicals can be influenced by the solvents, and the surrounding medium can lead to a change in the position, intensity, and shape of absorption bands [62]. The results indicate a significant dependence of the emission characteristics on the solvent polarity. Compound **(4b)** was chosen to investigate the solvatofluorochromism of the synthesized poly-fused heterocycles. The optical and photophysical properties of **(4b)** has been studied in commonly used organic solvents such as DMF, DMSO, CH_3CN, $CHCl_3$, MeOH, EtOH and H_2O. The fluorescence intensity maxima were found to vary with the nature of the solvent, which can be attributed to solvatochromic properties [63]. As it can be seen in Fig. 5, the fluorescent intensity of compound **(4b)** in DMF, CH_3CN, DMSO as aprotic solvents were ranked from first to third in comparison with the protic ones, respectively. These solvents do not have hydrogen bond with the solute and the spectrum of the solute closely approximates the spectrum that would be produced in the gaseous state, in which fine structure is often observed. Contrary to aprotic solvents, EtOH, MeOH and H_2O as protic solvents form hydrogen bond with solute and the fine structure may disappear.

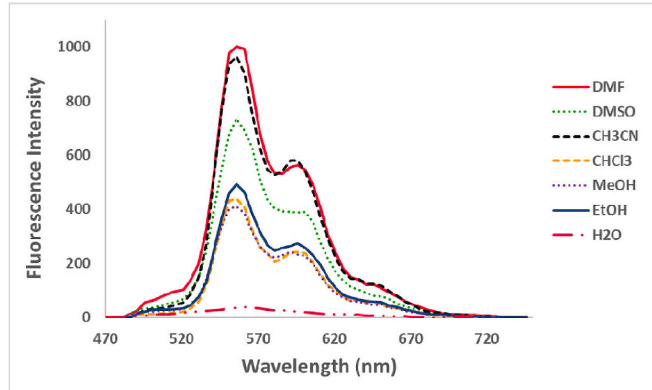

Fig. 5. Fluorescence intensity of a solution of compound **(4b)** (2×10^{-6} M) in the solvents DMF, DMSO, CH_3CN, $CHCl_3$, MeOH, EtOH, and H_2O at $\lambda_{ex.}$ = 471 nm.

2.4. Biological evaluation

2.4.1. In vitro antioxidant study

Based on the literature survey, antioxidant activity of *N*-(4-methyl-2-nitrophenyl)-2-(3-methyl-2-oxoquinoxalin-1(2*H*)-yl)acetamide have been studied via DPPH or 2,2-azinobis-(3-ethylbenzthiazolin-6-sulfonic acid (ABTS) free radical scavenging, ferric reducing power assay, and hydrogen peroxide scavenging activity methods [64]. Excellent antioxidant properties were observed with it compared to the same quinoxalines and positive control vitamin C. As expected, it showed competitive *in vitro* antidiabetic activities against *α*-glucosidase and *α*-amylase enzymes. Also, some (*E*)-6-((2-phenylhydrazono)methyl)quinoxaline derivatives were synthesized as potent antioxidant and antifungal agents [65]. The strongest antioxidant activities were observed with two derivatives according to EC_{50} values of 0.96 and 7.60 μg ml^{-1} recorded via mice microsome lipid peroxidation (LPO) and DPPH free radical scavenging methods.

Therefore, in our project, 2,2-diphenyl-1-picrylhydrazyl (DPPH) and ascorbic acid (vitamin C) were supplied from Sigma-Aldrich, and used without further purification. The *in vitro* antioxidant activity of methanolic solutions of the synthesized compounds **(3 & 4a-e)** and DPPH were determined at 517 nm using UV–Vis spectrophotometer (UV-2100 RAY Leigh, Beijing, China). DPPH free radical scavenging was assessed according to the previously published research [66].

Reactive oxygen species (ROS) generated by metabolic redox reactions can damage vital organs of plants and animals. These oxidative stresses cause a wide range of diseases, so that antioxidants trap the ROS and greatly reduce the risk of neurodegenerative, cardiovascular and diabetes diseases as well as the stroke prevention [67].

Consequently, hydrogen-atom donation of the synthesized poly-

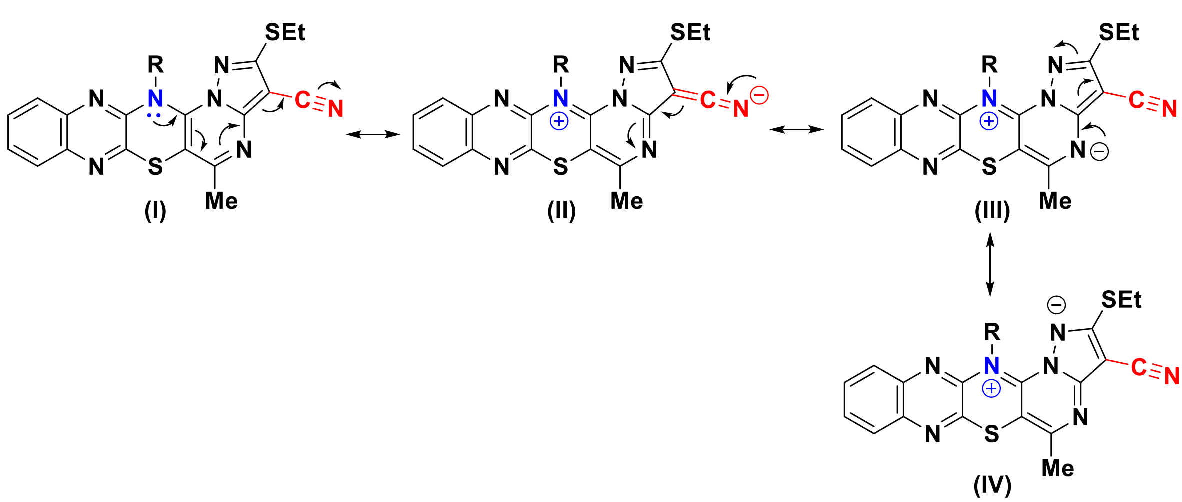

Scheme 3. Plausible intramolecular charge transfer and push-pull mechanism of donor-π-acceptor (D-π-A) novel fused pentacyclic dyes **(4a-e)**.

fused heterocycles **(3 & 4a-e)** were evaluated against free radical DPPH, and the results were reported as IC_{50} values in Table 2. Ascorbic acid (Vitamin C) was also applied as the standard.

Good to excellent antioxidant activities were observed with all synthetic derivatives **(3 & 4a-e)**. Since these compounds differ only in the nature of the 13-*N*-substitution, the *H*-atom donation must have been occurred in this position (Fig. 6).

Compound **(4e)** containing 13-benzyl substituent showed the best antioxidant property among the synthesized derivatives due to the presence of adjacent radical stabilizing phenyl group. Radical stabilizing groups on benzyl substituent can improve antioxidant capacities of compound **(4e)**. As the alkyl chain length increases from methyl to butyl in derivatives **(4a-d)**, the corresponding antioxidant activity decreases. In conclusion, introduction of benzyl substituent containing radical stabilizing groups on *N*-13 position may improve antioxidant potentials.

2.4.2. Antiproliferative study

Doxorubicin (Dox) is a highly effective medication for breast cancer chemotherapy, however, its toxic side effects on normal tissues, especially on myocardial cells, makes certain and limitation about its clinical application [68,69]. Furthermore, its administration is associated with the development of dose-dependent, irreversible, cumulative, and long-lasting cardiotoxic side effects. It is confirmed that Dox has other serious side effects, include; hair loss, rash, bone marrow suppression and vomiting. Unfortunately, there is no treatment for the toxic effect of DOX on DNA or to block these side effects. For this reason, scientists are looking for developing a new drug to replace DOX [70].

In this study, the significant cytotoxicity of the synthesized pyrazolo [5″,1'':2′,3']pyrimido[4′,5':5,6][1,4]thiazino[2,3-*b*]quinoxalins **(3 & 4a-e)** on MCF-7 breast cancer cells and cell line L929 (fibroblast) through assessment of their viabilities employing MTT assay protocol (*in vitro* tetrazolium-based colorimetric assay) was investigated for certain time intervals [71–73] and presented as IC_{50} values (the half maximal-inhibitory concentrations) in Tables 3 and 4. Doxorubicin used as a standard drug to compare the anti-proliferative properties of all the newly synthesized compounds with those of standard clinical medicines. MCF-7 cancer cells were exposed to various concentrations of the doxorubicin at 24, 48 and 72 h (Table 3) [72,74].

Amongst the heterocyclic compounds used in this screening, **(4e)** bearing *N*-benzyl and **(4b)** bearing *N*-Ethyl on the *N*-13 position of pyrazolo[5″,1'':2′,3']pyrimido[4′,5':5,6][1,4]thiazino[2,3-*b*]quinoxaline skeleton with IC_{50} values of 0.2 mM and 0.37 mM were ranked in the first and second places of cytotoxicity against MCF-7 cells after 72 h treatment, respectively. While, N^{13}-propyl substituted **(4c)** as the least effective compound showed IC_{50} value of 1.3 mM after 72 h. The graphs of dose-dependent cytotoxicity of compounds **(4a-e)** on MCF-7 cell are depicted in Fig. 7.

All the pentacyclic derivatives affected on normal L929 cell line to determine their IC_{50} values (Table 4). These compounds do not have high cytotoxicity on L929 cell line. This phenomenon can be attributed to the increased accumulation of the mentioned compounds in cancer cells. As a result, cancer cells have a higher tendency to absorb more amount of each compound, which ultimately leads to the death of cancerous cells. The graphs of dose-dependent cytotoxicity of compounds **(4a-e)** on L929 cell are depicted in Fig. 8.

Totally, because the newly synthesized compounds (especially **(4b)** and **(4e)**) showed suitable anticancer effects on MCF7 cell line, and their toxicities were not high significant on normal fibroblast cells, further investigation on them is worthy. Therefore, more research like *in vivo* and molecular tests studies can be design on these compounds in future to determine the anticancer mechanisms and *in vivo* toxicity.

2.5. Conclusion

In summary, we have successfully developed an efficient and convenient synthesis of potential pharmacologically active and fluorescent derivatives of a novel fused five cyclic scaffold, pyrazolo [5″,1'':2′,3']pyrimido[4′,5':5,6][1,4]thiazino[2,3-*b*]quinoxaline, by employing a one-pot heterocyclization/*N*-alkylation domino reaction of

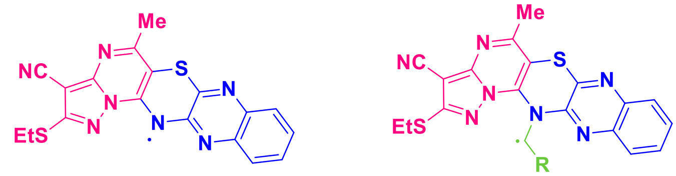

Fig. 6. The initial radicals probably formed by the interaction with DPPH radical.

Table 3
The cytotoxicity effects of pyrazolo[5″,1'':2′,3']pyrimido[4′,5':5,6][1,4]thiazino[2,3-*b*]quinoxalins **(4a-e)** on MCF-7 determined by MTT assay.

Compounds	IC_{50} (mM) ± SD[a] MCF7 cells		
	24 h	48 h	72 h
(4a)	1.09 ± 0.2	0.8 ± 0.09	0.64 ± 0.06
[b](4b)	0.57 ± 0.02	0.46 ± 0.03	0.37 ± 0.07
(4c)	2.44 ± 0.02	1.6 ± 0.04	1.3 ± 0.09
(4d)	0.94 ± 0.08	0.66 ± 0.08	0.47 ± 0.08
[b](4e)	0.39 ± 0.01	0.30 ± 0.02	0.2 ± 0.04
Doxorubicin	0.042 ± 0.02	0.022 ± 0.05	0.016 ± 0.01

[a] The IC_{50} values are shown as mean ± SD (n = 3).
[b] Lowest IC_{50}.

Table 4
The cytotoxicity effects of pyrazolo[5″,1'':2′,3']pyrimido[4′,5':5,6][1,4]thiazino[2,3-*b*]quinoxalins **(4a-e)** on L929 determined by MTT assay.

Compounds	IC_{50} (mM) ± SD[a] L929 cells		
	24 h	48 h	72 h
(4a)	2.316 ± 0.9	2.151 ± 0.4	1.244 ± 0.8
(4b)	1.518 ± 0.9	0.855 ± 0.3	0.696 ± 0.05
(4c)	1.651 ± 0.78	1.021 ± 0.19	0.777 ± 0.12
(4d)	2.610 ± 0.8	2.165 ± 0.20	1.795 ± 0.6
(4e)	1.410 ± 0.22	0.861 ± 0.33	0.624 ± 0.4
Doxorubicin	0.026 ± 0.004	0.019 ± 0.003	0.017 ± 0.002

[a] The IC_{50} values are shown as mean ± SD (n = 3).

Table 2
Antioxidant activity of compounds **(3 & 4a-e)**.

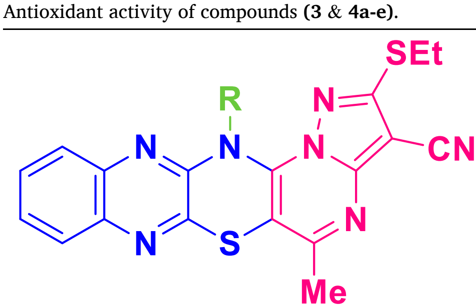

Compound	R	DPPH IC_{50} (μM)
(3)	H	46
(4a)	Me	33
(4b)	Et	41
(4c)	*n*-Pr	60
(4d)	*n*-Bu	71
(4e)	Bn	29
Vitamin C	–	22

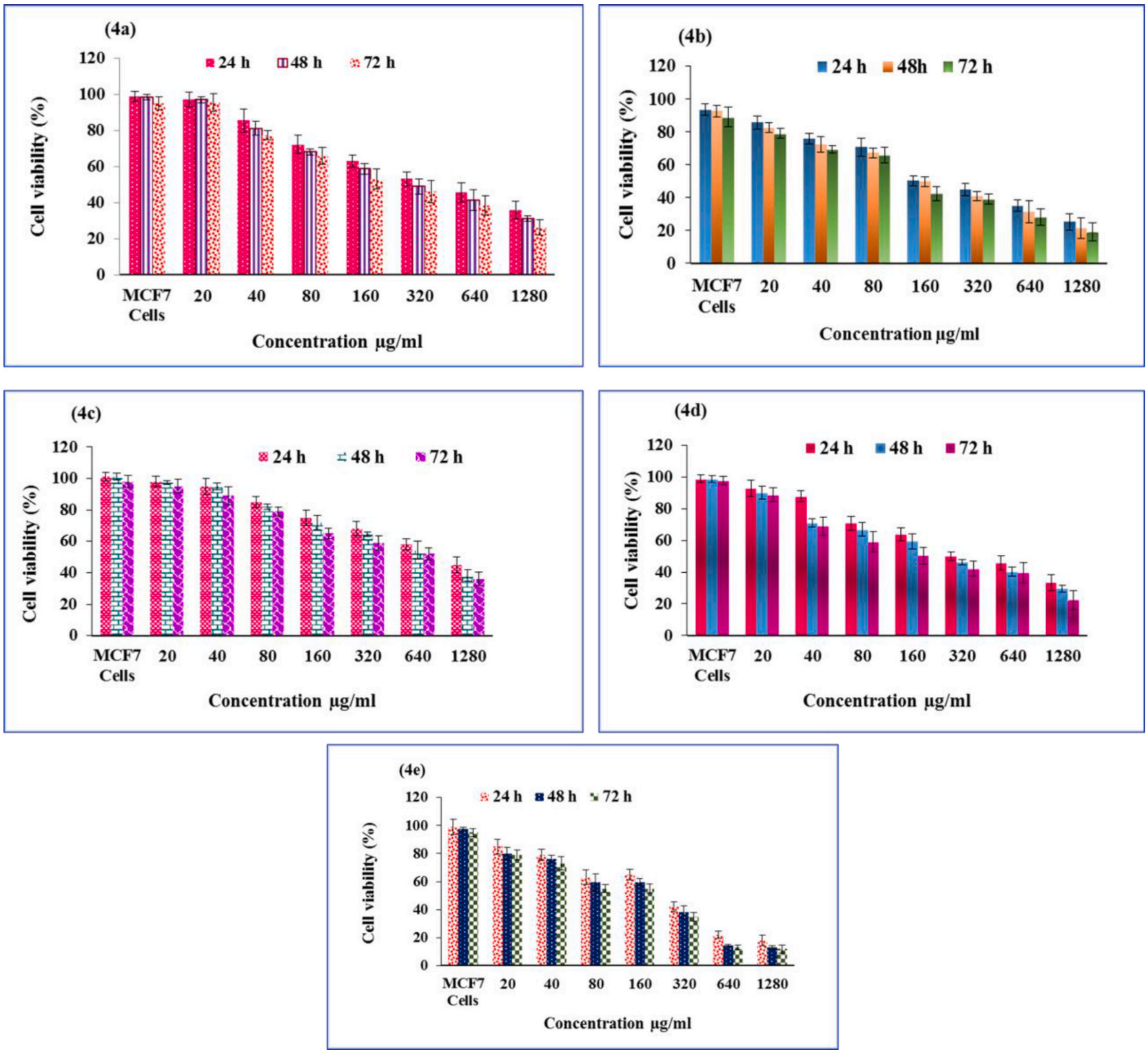

Fig. 7. The cytotoxicity of pyrazolo[5″,1’’:2′,3’]pyrimido[4′,5’:5,6][1,4]thiazino[2,3-*b*]quinoxalins **(4a-e)** on MCF-7 cells at 24, 48 and 72 h. Results are mean ± SD (n = 3).

6-bromo-7-chloro-2-(ethylthio)-5-methylpyrazolo[1,5-*a*]pyrimidine-3-carbonitrile with 3-aminoquinoxaline-2-thiol and various alkyl halides in the presence of potassium carbonate in *N,N*-dimethyl formamide at 80–90 °C. The photophysical, *H*-atom donating potentials against DPPH radical and cytotoxicity against MCF-7 breast cancerous cells for all the newly synthesized heterocycles were screened precisely. Taking into account the strongest antioxidant and antiproliferative activities of *N*-Benzylated derivative **(4e)** as well as large Stokes shift and very high quantum yield of **(3)** derivative and in view of the less toxicity of compounds on normal fibroblast L929 cells, these potent compounds can present a new platform for synthesis of novel florescent biologically active probs with strong antioxidant and anticancer activities. Introduction of benzyl substituent containing radical stabilizing groups on *N*-13 position may improve their antioxidant potentials as well as anticancer properties.

2.6. Experimental

Melting points were recorded on an Electro thermal type 9200 melting point apparatus. The IR spectra were obtained on Avatar 370 FT-IR Thermo Nicolet and only noteworthy absorptions are listed. The ^{1}H NMR (300 MHz) and the ^{13}C NMR (75 MHz) spectra were recorded on a Bruker Avance-III 300 nmr Fourier transformer spectrometer. Chemical shifts are reported in ppm downfield from TMS as internal standard. The mass spectra were scanned on a Varian Mat CH-7 at 70 eV. High-resolution ESI mass spectra were recorded on an Agilent 6220 Accurate Mass TOF LC/MS spectrometer. Elemental analyses were performed on a Thermo Finnigan Flash EA microanalyzer.

2.6.1. Synthesis of 3-aminoquinoxaline-2-thiol (1)

Compound (1) was prepared by the literature procedure [37]. Yellow powder; yield = 73%; mp: > 300 °C; ^{1}H NMR (300 MHz, DMSO-d_6): δ 7.02 (s, 2H, –NH$_2$), 7.23–7.45 (m, 4H, Ar–H), 14.33 (s, 1H, –SH) ppm; ^{13}C NMR (75 MHz, DMSO-d_6): δ 115.9, 124.7125.0, 126.5, 128.2, 136.5, 154.3, 168.2 ppm; IR (KBr disc): ν 3395, 3264, 1450, 1359 cm^{-1}; MS (*m/z*) 177 (M^{+}). Anal. calcd for $C_8H_7N_3S$ (%): C, 54.22; H, 3.98; N, 23.71; S, 18.09; Found: C, 54.18; H, 3.92; N, 23.63; S, 18.05.

2.6.2. *Synthesis of 6-bromo-7-chloro-3-cyano-2-(ethylthio)-5-methylpyrazolo[1,5-a]pyrimidine (2)*

6-Bromo-3-cyano-2-(ethylthio)-5-methyl-7-oxo-6,7-dihydropyrazolo[1,5-*a*]pyrimidine (1.56 g, 5 mmol) was refluxed in $POCl_3$ (10 ml) for 48 h. After the completion of the reaction (monitored by TLC, *n*-Hexane:EtOAc, 8:2), the mixture was added to an ice–water bath and neutralized with saturated $NaHCO_3$ solution. The resulting solid was filtered off, washed with cold water (2 × 50 ml) and dried at room

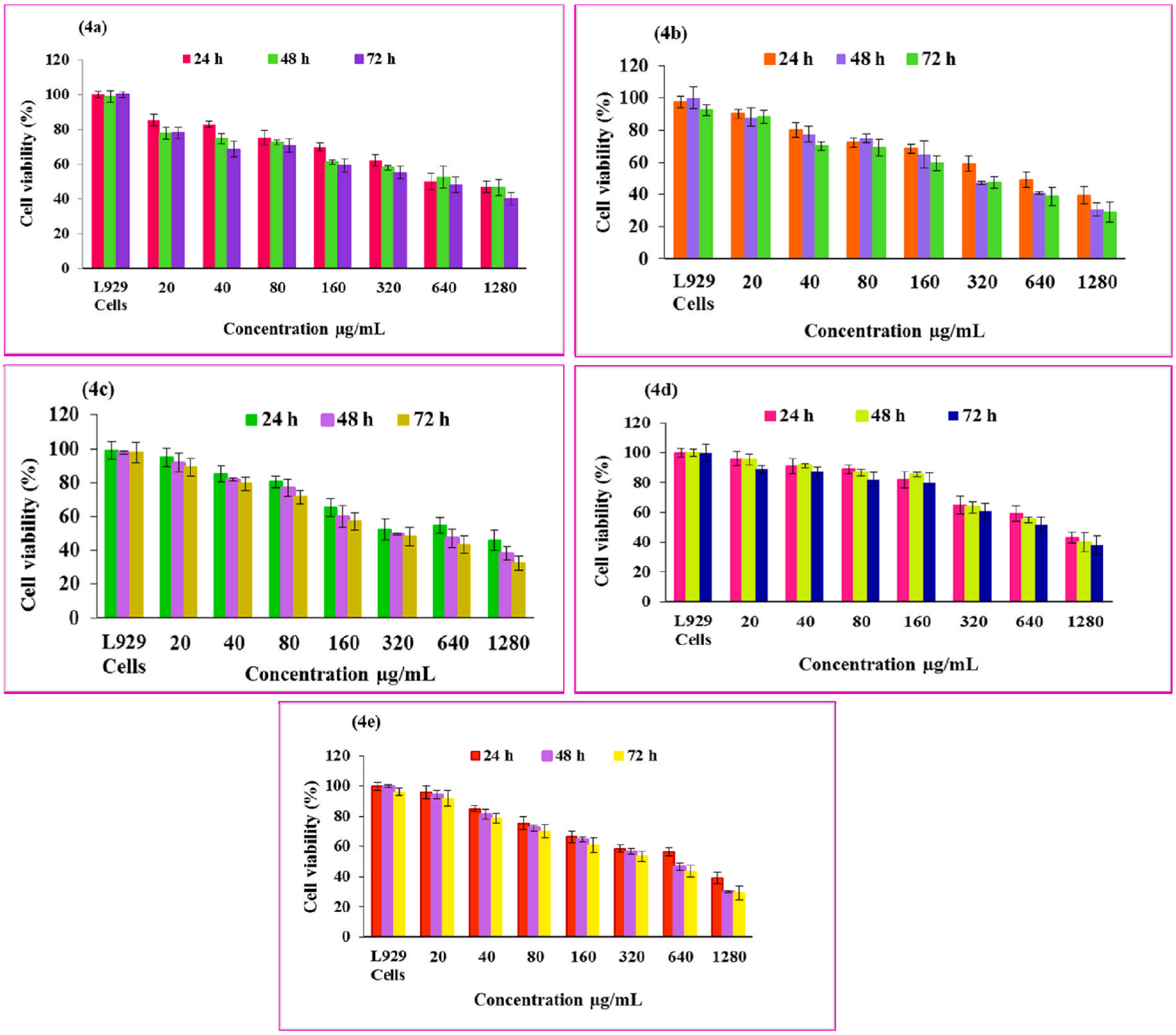

Fig. 8. The cytotoxicity of pyrazolo[5″,1’’:2′,3’]pyrimido[4′,5’:5,6][1,4]thiazino[2,3-*b*]quinoxalins **(3 & 4a-e)** on L929 normal cells at 24, 48 and 72 h. Results are mean ± SD (n = 3).

temperature [35]. Brown powder; yield = 89%; mp: 182–184 °C; ^{1}H NMR (300 MHz, $CDCl_3$): *δ* 1.32 (t, 3H, *J* = 7.6 Hz, –CH_3), 2.11 (s, 3H, –CH_3), 2.46 (q, 2H, *J* = 7.6 Hz, –SCH_2) ppm; ^{13}C NMR (75 MHz, $CDCl_3$): *δ* 14.3, 23.2, 23.5, 89.9, 117.0, 119.6, 148.3, 150.5, 161.0, 164.4 ppm; IR (KBr disc): *ν* 2962, 2929, 2223 (CN), 1595, 1468, 918 (C–Cl), 718 (C–Br) cm^{-1}; MS (*m/z*) 331 (M^+), 302 (M^+-Et), 296 (M^+ − Cl), 270 (M^+ − SEt). Anal. Calcd. for $C_{10}H_8BrClN_4OS$ (%): C, 36.22; H, 2.43; N, 16.89; S, 9.67; Found: C, 36.17; H, 2.39; N, 16.85; S, 9.64.

2.6.3. Synthesis of 3-cyano-2-(ethylthio)-5-methyl-13H-pyrazolo [5″,1’’:2′,3’]pyrimido[4′,5’:5,6][1,4]thiazino[2,3-b]quinoxaline (3)

To a mixture of 3-aminoquinoxaline-2-thiol **(1)** (1 mmol, 0.177 g) and compound **(2)** (1 mmol, 0.331 g) in DMF (3 ml), K_2CO_3 (2 mmol, 0.227 g) was added and the mixture was heated at 80–90 °C for 90 min. After the completion of the reaction, the mixture was cooled, poured into an ice/water bath and neutralized with aqueous 5% HCl solution. The resulting solid product was collected by filtration and recrystallized from ethanol.

Light brown powder; yield = 87%; mp: > 350 °C; ^{1}H NMR (300 MHz, DMSO-d_6): *δ* 1.29 (t, 3H, *J* = 7.3 Hz, –CH_3), 2.00 (s, 3H, –CH_3), 3.17 (q, 2H, *J* = 7.3 Hz, –SCH_2), 7.01–7.37 (m, 4H, Ar–H) ppm; ^{13}C NMR (75 MHz, DMSO-d_6): *δ* 15.0, 21.9, 25.3, 76.4, 96.4, 115.0, 125.8, 126.1, 126.3, 128.5, 139.6, 142.5, 147.4, 149.9, 151.9, 153.2, 153.9 ppm; IR (KBr disc): *ν* 3347, 3056, 2962, 2925, 2213 (CN), 1594, 1554, 1454, 1394, 1276, 1208, 744 cm^{-1}; MS (*m/z*) 391 [M^+]. HRMS Calcd for $C_{18}H_{14}N_7S_2$ $[M+H]^+$: 392.0747; Found: 392.0752. Anal. Calcd. for $C_{18}H_{13}N_7S_2$ (%): C, 55.23; H, 3.35; N, 25.05; S, 16.38; Found: C, 55.21; H, 3.33; N, 25.00; S, 16.33.

2.6.4. Synthesis of N-alkylated pyrazolo[5″,1’’:2′,3’]pyrimido [4′,5’:5,6][1,4]thiazino[2,3-b]quinoxalines (4a-e); general procedure

To a mixture of 3-aminoquinoxaline-2-thiol **(1)** (1 mmol, 0.177 g) and compound **(2)** (1 mmol, 0.331 g) in DMF (3 ml), K_2CO_3 (2 mmol, 0.227 g) was added and the mixture was heated at 80–90 °C for 90 min. After the completion of the reaction (monitored by TLC, $CHCl_3$:MeOH, 20:1), an excess amount of the appropriate alkyl halide (0.3 ml) was added and the mixture was heated at 80–90 °C for 2 h more. After the completion of the reaction, the mixture was cooled, poured into an ice/water bath and neutralized with aqueous 5% HCl solution. The resulting solid product was collected by filtration and recrystallized from ethanol.

Due to their very low solubility, no satisfying ^{13}C NMR spectrum was obtained even with long time accumulation.

3-Cyano-2-(ethylthio)-5,13-dimethyl-13*H*-pyrazolo [5″,1’’:2′,3’] pyrimido [4′,5’:5,6] [1,4] thiazino [2,3-*b*] quinoxaline (4a): (The alkyl halide is CH_3I). Dark red powder; yield = 87%; mp: > 350 °C; ^{1}H NMR (300 MHz, Acetone-d_6): *δ* 1.38 (t, 3H, *J* = 7.3 Hz, –CH_3), 2.45 (s, 3H, –CH_3), 3.25 (q, 2H, *J* = 7.3 Hz, –SCH_2), 3.96 (q, 3H, –NCH_3), 7.51–7.60 (m, 2H, Ar–H), 7.71 (ddd, 2H, *J* = 7.4, 4.5, 1.6 Hz, Ar–H) ppm; IR (KBr disc): *ν* 3068, 2958, 2917, 2868, 2214 (CN), 1596, 1517, 1452, 1408, 1362, 1283, 1179, 1086, 927, 772 cm^{-1}; MS *(m/z)* 405 [M^+]. HRMS Calcd for $C_{19}H_{16}N_7S_2$ $[M+H]^+$: 406.0903; Found: 406.0895. Anal. Calcd. for $C_{19}H_{15}N_7S_2$ (%):C, 56.28; H, 3.73; N, 24.18; S, 15.81; Found: C, 56.24; H, 3.70; N, 24.11; S, 15.76.

3-Cyano-13-ethyl-2-(ethylthio)-5-methyl-13*H*-pyrazolo [5″,1'':2′,3'] pyrimido [4′,5′:5,6] [1,4] thiazino [2,3-*b*] quinoxaline (4b): (The alkyl halide is C_2H_5I). Dark red powder; yield = 86%; mp: >350 °C; ^{1}H NMR (300 MHz, Acetone-d_6): δ 1.32 (t, 3H, J = 7.0 Hz, –CH_3), 1.37 (t, 3H, J = 7.3 Hz, –CH_3), 2.48 (s, 3H, –CH_3), 3.26 (q, 2H, J = 7.3 Hz, –SCH_2), 4.80 (q, 2H, J = 7.0 Hz, –NCH_2), 7.51–7.62 (m, 2H, Ar–H), 7.73 (ddd, 2H, J = 7.6, 4.0, 1.6 Hz, Ar–H) ppm; IR (KBr disc): ν 3060, 2947, 2928, 2868, 2218 (CN), 1594, 1518, 1443, 1303, 1283, 1095, 762 cm^{-1}; MS *(m/z)* 419 [M^+]. HRMS Calcd for $C_{20}H_{18}N_7S_2$ $[M+H]^+$: 420.1060; Found: 420.1071. Anal. Calcd. for $C_{20}H_{17}N_7S_2$ (%): C, 57.26; H, 4.08; N, 23.37; S, 15.28; Found: C, 57.23; H, 4.02; N, 23.35; S, 15.24.

3-Cyano-2-(ethylthio)-5-methyl-13-propyl-13*H*-pyrazolo [5″,1'':2′,3'] pyrimido [4′,5′:5,6] [1,4] thiazino [2,3-*b*] quinoxaline (4c): (The alkyl halide is *n*-C_3H_7Br). Dark red powder; yield = 78%; mp: 344–346 °C; ^{1}H NMR (300 MHz, D_3PO_4/D_2O): δ 0.68 (t, 3H, J = 7.0 Hz, –CH_3), 1.13 (t, 3H, J = 7.3 Hz, –CH_3), 1.46 (m, 2H, J = 7.0 Hz, –CH_2), 2.45 (s, 3H, –CH_3), 3.06 (q, 2H, J = 7.3 Hz, –SCH_2), 3.87 (t, 3H, J = 7.0 Hz, –NCH_2), 6.98–7.22 (m, 4H, Ar–H) ppm; IR (KBr disc): ν 3064, 3011, 2964, 2925, 2872, 2215 (CN), 1594, 1516, 1444, 1377, 1283, 1097, 934, 775, 760 cm^{-1}; MS *(m/z)* = 433 [M^+]. HRMS Calcd for $C_{21}H_{20}N_7S_2$ $[M+H]^+$: 434.1216; Found: 434.1212. Anal. Calcd. for $C_{21}H_{19}N_7S_2$ (%): C, 58.18; H, 4.42; N, 22.62; S, 14.79; Found: C, 58.15; H, 4.40; N, 22.58; S, 14.76.

13-Butyl-3-cyano-2-(ethylthio)-5-methyl-13*H*-pyrazolo [5″,1'':2′,3'] pyrimido [4′,5′:5,6] [1,4] thiazino [2,3-*b*] quinoxaline (4d): (The alkyl halide is *n*-C_4H_9Br). Dark red powder; yield yield = 71%; mp: 318–320 °C; ^{1}H NMR (300 MHz, D_3PO_4/D_2O): δ 0.60 (t, 3H, J = 7.0 Hz, –CH_3), 1.06 (m, 5H), 1.36 (m, 2H, –CH_2), 2.44 (s, 3H, –CH_3), 2.95 (q, 2H, J = 7.3 Hz, –SCH_2), 3.86 (t, 3H, J = 7.0 Hz, –NCH_2), 6.98–7.22 (m, 4H, Ar–H) ppm; IR (KBr disc): ν 3060, 2961, 2929, 2868, 2215 (CN), 1594, 1511, 1439, 1379, 1284, 1178, 1097, 925, 774, 760 cm^{-1}; MS *(m/z)* = 447 [M^+]. HRMS Calcd for $C_{22}H_{22}N_7S_2$ $[M+H]^+$: 448.1373; Found: 448.1370. Anal. Calcd. for $C_{22}H_{21}N_7S_2$ (%): C, 59.04; H, 4.73; N, 21.91; S, 14.33; Found: C, 59.00; H, 4.70; N, 21.87; S, 14.29.

13-Benzyl-3-cyano-2-(ethylthio)-5-methyl-13*H*-pyrazolo [5″,1'':2′,3'] pyrimido [4′,5′:5,6] [1,4] thiazino [2,3-*b*] quinoxaline (4e): (The alkyl halide is $PhCH_2Br$). Dark red powder; yield = 67%; mp: 313–315 °C; ^{1}H NMR (300 MHz, D_3PO_4/D_2O): δ 1.02 (t, 3H, J = 7.3 Hz, –CH_3), 2.45 (s, 3H, –CH_3), 2.93 (q, 2H, J = 7.3 Hz, –SCH_2), 5.04 (s, 2H, –NCH_2), 6.82–7.02 (m, 9H, Ar–H) ppm; IR (KBr disc): ν 2973, 2924, 2214 (CN), 1595, 1520, 1450, 1286, 1274, 1103, 757 cm^{-1}; MS *(m/z)* 482 (M^+). Anal. Calcd. for $C_{25}H_{19}N_7S_2$ (%): C, 62.35; H, 3.98; N, 20.36; S, 13.31; Found: C, 62.33; H, 3.93; N, 20.30; S, 13.29.

Credit author Statement

S. Sheikhi-Mohammareh and A. Shiri conceived and planned the experiments including organic synthesis and photophysical study. S. Sheikhi-Mohammareh carried out the experiments. A. Salimi, S. Sheikhi-Mohammareh and A. Shiri planned PXRD analysis and contributed to the interpretation of the results. H. Beyzaei and M. Moghaddam-Manesh carried out *in vitro* antioxidant study and H. Beyzaei, M. Moghaddam-Manesh and S. Sheikhi-Mohammareh contributed to the interpretation of the results. F. Oroojalian and F. Azizollahi carried out anti-proliferative study and S. Sheikhi-Mohammareh and F. Oroojalian contributed to the interpretation of the results. S. Sheikhi-Mohammareh took the lead in writing the manuscript. S. Sheikhi-Mohammareh and A. Shiri provided critical feedback and helped shape the research, analysis and manuscript.

Declaration of competing interest

The authors declare that they have no known competing financial interests or personal relationships that could have appeared to influence the work reported in this paper.

Data availability

No data was used for the research described in the article.

Acknowledgment

The authors gratefully acknowledge Research Council of Ferdowsi University of Mashhad for financial support of this project (3/44510).

Appendix. ASupplementary data

Supplementary data to this article can be found online at https://doi.org/10.1016/j.talanta.2023.124723.

References

[1] S.A. Khan, K. Saleem, Z. Khan, Synthesis, characterization and in vitro antibacterial activity of new steroidal thiazolo quinoxalines, Eur. J. Med. Chem. 42 (2007) 103–108, https://doi.org/10.1016/j.ejmech.2006.07.006.
[2] V.K. Tandon, D.B. Yadav, H.K. Maurya, A.K. Chaturvedi, P.K. Shukla, Design, synthesis, and biological evaluation of 1,2,3-trisubstituted-1,4-dihydrobenzo[g] quinoxaline-5,10-diones and related compounds as antifungal and antibacterial agents, Bioorg. Med. Chem. 14 (2006) 6120–6126, https://doi.org/10.1016/j.bmc.2006.04.029.
[3] A.A. Abu-Hashem, M.A. Gouda, F.A. Badria, Eur. J. Med. Chem. (2010).
[4] M.R. Islami, Z. Hassani, One-pot and efficient protocol for synthesis of quinoxaline derivatives, ARKIVOC (Gainesville, FL, U. S.) 2008 (2008) 280–287.
[5] C. Srinivas, C.N.S.S.P. Kumar, V.J. Rao, S. Palaniappan, Green approach for the synthesis of quinoxaline derivatives in water medium using reusable polyaniline-sulfate salt catalyst and sodium laurylsulfate, Catal. Lett. 121 (2008) 291–296.
[6] H.M. Bachhav, S.B. Bhagat, V.N. Telvekar, Efficient protocol for the synthesis of quinoxaline, benzoxazole and benzimidazole derivatives using glycerol as green solvent, Tetrahedron Lett. 52 (2011) 5697–5701.
[7] I.A.I. Ali, I.A. Al-Masoudi, H.G. Hassan, N.A. Al-Masoudi, Synthesis and anti-HIV activity of new homo acyclic nucleosides, 1-(pent-4-enyl) quinoxalin-2-ones and 2-(pent-4-enyloxy) quinoxalines, Chem. Heterocycl. Compd. 43 (2007) 1052–1059.
[8] A. Gazit, K. Yee, A. Uecker, F.D. Böhmer, T. Sjöblom, A. Östman, J. Waltenberger, G. Golomb, S. Banai, M.C. Heinrich, A. Levitzki, Tricyclic quinoxalines as potent kinase inhibitors of PDGFR kinase, Flt3 and Kit, Bioorg. Med. Chem. 11 (2003) 2007–2018, https://doi.org/10.1016/S0968-0896(03)00048-8.
[9] S. Schwarz, C. Kehrenberg, T.R. Walsh, Use of antimicrobial agents in veterinary medicine and food animal production, Int. J. Antimicrob. Agents 17 (2001) 431–437.
[10] M.M. Heravi, K. Bakhtiari, F.F. Bamoharram, M.H. Tehrani, Wells-Dawson type heteropolyacid catalyzed synthesis of quinoxaline derivatives at room temperature, Monatshefte Für Chemie-Chemical Mon 138 (2007) 465–467.
[11] A. Kumar, S. Kumar, A. Saxena, A. De, S. Mozumdar, Ni-nanoparticles, An efficient catalyst for the synthesis of quinoxalines, Catal. Commun. 9 (2008) 778–784, https://doi.org/10.1016/j.catcom.2007.08.021.
[12] K.R. Justin Thomas, M. Velusamy, J.T. Lin, C.-H. Chuen, Y.-T. Tao, Chromophore-labeled quinoxaline derivatives as efficient electroluminescent materials, Chem. Mater. 17 (2005) 1860–1866.
[13] Y. Yamashita, Organic semiconductors for organic field-effect transistors, Sci. Technol. Adv. Mater. 10 (2009), 24313.
[14] H.M. Meshram, G.S. Kumar, P. Ramesh, B.C. Reddy, A mild and convenient synthesis of quinoxalines via cyclization–oxidation process using DABCO as catalyst, Tetrahedron Lett. 51 (2010) 2580–2585.
[15] M.M. Heravi, B. Baghernejad, H.A. Oskooie, A novel three-component reaction for the synthesis of N-cyclohexyl-3-aryl-quinoxaline-2-amines, Tetrahedron Lett. 50 (2009) 767–769.
[16] P.P. Castro, G. Zhao, G.A. Masangkay, C. Hernandez, L.M. Gutierrez-Tunstad, Quinoxaline excision: a novel approach to tri-and diquinoxaline cavitands, Org. Lett. 6 (2004) 333–336.
[17] K. Aravind, A. Ganesh, D. Ashok, Microwave assisted synthesis, characterization and antibacterial activity of quinoxaline derivatives, J. Chem. Pharmaceut. Res. 5 (2013) 48–52.
[18] P. Haldar, B. Dutta, J. Guin, J.K. Ray, Uncatalyzed condensation between aryl-1, 2-diamines and diethyl bromomalonate: a one-pot access to substituted ethyl 3-hydroxyquinoxaline-2-carboxylates, Tetrahedron Lett. 48 (2007) 5855–5857.
[19] J.F. Zhou, G.-X. Gong, L.-T. An, Y. Liu, F.-X. Zhu, Y.-L. Zhu, S.-J. Ji, An efficient synthesis of quinoxalines under catalyst-free and microwave-irradiation conditions, Synlett (2008) (2008) 3163–3166.

[20] Y.A. Sonawane, R.N. Rajule, G.S. Shankarling, Synthesis of novel diphenylamine-based fluorescent styryl colorants and study of their thermal, photophysical, and electrochemical properties, Monatshefte Für Chemie-Chemical Mon 141 (2010) 1145–1151.
[21] D. Aparicio, O.A. Attanasi, P. Filippone, R. Ignacio, S. Lillini, F. Mantellini, F. Palacios, J.M. de Los Santos, Straightforward access to pyrazines, piperazinones, and quinoxalines by reactions of 1, 2-diaza-1, 3-butadienes with 1, 2-diamines under solution, solvent-free, or solid-phase conditions, J. Org. Chem. 71 (2006) 5897–5905.
[22] S.K. Singh, P. Gupta, S. Duggineni, B. Kundu, Solid phase synthesis of quinoxalines, Synlett 2003 (2003) 2147–2150.
[23] P. Panneerselvam, R.S. Reddy, K. Murali, N.R. Kumar, Synthesis, analgesic, anti-inflammatory and antimicrobial activities of some novel Schiff's bases of 5-subsituted Isatin, Der Pharma Chem. 2 (2010) 28–37.
[24] J. Mazumdera, R. Chakraborty, S. Sena, S. Vadrab, B. Dec, T.K. Ravi, Synthesis and biological evaluation of some novel quinoxalinyl triazole derivatives, Der Pharma Chem. 1 (2009) 188–198.
[25] M. Bakavoli, H. Eshghi, H. Azizollahi, S. Saberi, F. Bazrafshan, One-pot, procedure for the preparation of some thiazino [2, 3-b] quinoxaline derivatives, J. Chem. Res. 38 (2014) 189–191.
[26] A. V Ivachtchenko, E.S. Golovina, M.G. Kadieva, V.M. Kysil, O.D. Mitkin, S. E. Tkachenko, I.M. Okun, Synthesis and structure–activity relationship (SAR) of (5, 7-disubstituted 3-phenylsulfonyl-pyrazolo [1, 5-a] pyrimidin-2-yl)-methylamines as potent serotonin 5-HT6 receptor (5-HT6R) antagonists, J. Med. Chem. 54 (2011) 8161–8173.
[27] A. Damont, V. Médran-Navarrete, F. Cacheux, B. Kuhnast, G. Pottier, N. Bernards, F. Marguet, F. Puech, R. Boisgard, F. Dollé, Novel pyrazolo [1, 5-a] pyrimidines as translocator protein 18 kDa (TSPO) ligands: synthesis, in vitro biological evaluation,[18F]-labeling, and in vivo neuroinflammation PET images, J. Med. Chem. 58 (2015) 7449–7464.
[28] J. Castillo-Sánchez, A. Aguilera-del Real, M. Rodriguez-Sánchez, A. Valverde-García, Residue levels, decline curves, and plantation distribution of procymidone in green beans grown in greenhouse, J. Agric. Food Chem. 48 (2000) 2991–2994.
[29] E. Sanna, F. Busonero, G. Talani, M. Carta, F. Massa, M. Peis, E. Maciocco, G. Biggio, Comp. Eff. Zaleplon, zolpidem, triazolam var. GABA A recept. Subtypes, Eur. J. Pharmacol. 451 (2002) 103–110.
[30] M.P. Martin, S.H. Olesen, G.I. Georg, E. Schonbrunn, Cyclin-dependent kinase inhibitor dinaciclib interacts with the acetyl-lysine recognition site of bromodomains, ACS Chem. Biol. 8 (2013) 2360–2365.
[31] L.J. Phillipson, D.H. Segal, T.L. Nero, M.W. Parker, S. San Wan, M. de Silva, M. A. Guthridge, A.H. Wei, C.J. Burns, Discovery and SAR of novel pyrazolo [1, 5-a] pyrimidines as inhibitors of CDK9, Bioorg, Med. Chem. 23 (2015) 6280–6296.
[32] X. Zhang, Y. Song, L. Gao, X. Guo, X. Fan, Highly facile and regio-selective synthesis of pyrazolo [1, 5-a] pyrimidines via reactions of 1, 2-allenic ketones with aminopyrazoles, Org. Biomol. Chem. 12 (2014) 2099–2107.
[33] H.A. Abdel-Aziz, T.S. Saleh, H.S.A. El-Zahabi, Facile synthesis and in-vitro antitumor activity of some pyrazolo [3, 4-b] pyridines and pyrazolo [1, 5-a] pyrimidines linked to a thiazolo [3, 2-a] benzimidazole moiety, Arch. Der Pharm. An Int. J. Pharm. Med. Chem. 343 (2010) 24–30.
[34] H.H. Abdel-Razik, A.A. Fadda, Synthesis of 1-(p-tosyl) pyrazolo [1, 5-a]-pyrimidines and pyrazolo [1, 5-c]-[1, 2, 4] triazine derivatives, Synth, Commun. Now. 31 (2001) 3547–3556.
[35] S. Sheikhi-Mohammareh, A. Shiri, M. Bakavoli, J. Mague, A straightforward approach for the synthesis of novel derivatives of benzo[b]pyrazolo[5′,1′:2,3] pyrimido[4,5-e][1,4]thiazine, J. Heterocycl. Chem. 53 (2016) 1231–1235, https://doi.org/10.1002/jhet.2432.
[36] J. Quiroga, J. Portilla, R. Abonia, B. Insuasty, M. Nogueras, J. Cobo, Regioselective synthesis of novel substituted pyrazolo [1, 5-a] pyrimidines under solvent-free conditions, Tetrahedron Lett. 49 (2008) 6254–6256.
[37] S. Sheikhi-mohammareh, A. Shiri, M. Bakavoli, Synthesis of new derivatives of pyrazolo [4 , 3- e][1 , 2 , 4] triazolo [4 , 3- c] pyrimidine, J. Chem. Res. 39 (2015) 403–406.
[38] S. Sheikhi-Mohammareh, A. Shiri, An alternative regioselective approach for the synthesis of highly functionalized derivatives of pyrazolo[5,1- b]purine scaffold, J. Heterocycl. Chem. 55 (2018) 2055–2060, https://doi.org/10.1002/jhet.3242.
[39] S. Sheikhi-Mohammareh, A. Shiri, H. Beyzaei, E. Yarmohammadi, New efficient design and synthesis of novel antioxidant and antifungal 7-imino[1,3]selenazolo [4,5-d]pyrimidine-5(4H)-thiones utilizing a base-promoted cascade addition/ cyclization sequence, Monatshefte Für Chemie - Chem. Mon. 151 (2020) 963–969, https://doi.org/10.1007/s00706-020-02617-2.
[40] S. Sheikhi-Mohammareh, A. Shiri, E.H. Maleki, M.M. Matin, H. Beyzaei, P. Baranipour, F. Oroojalian, T. Memariani, Synthesis of various derivatives of [1,3]Selenazolo[4,5-d]pyrimidine and exploitation of these heterocyclic systems as antibacterial, antifungal, and anticancer agents, ChemistrySelect 5 (2020) 10060–10066, https://doi.org/10.1002/slct.202002474.
[41] S. Sheikhi-Mohammareh, M. Mashreghi, A. Shiri, Robust approach leading to novel densely functionalized four-cyclic benzo[e]pyrazolo[5′,1′:2,3]pyrimido[4,5-b] [1,4]diazepines with antibacterial activity toward resistant strains, J. Iran. Chem. Soc. 17 (2020) 1555–1566, https://doi.org/10.1007/s13738-020-01875-5.
[42] O. Kohandel, S. Sheikhi, M. Fatemeh, T. Memariani, J. Mague, A Dimroth rearrangement approach for the synthesis activity on breast cancer cells, Mol. Divers. (2021), https://doi.org/10.1007/s11030-021-10290-8.
[43] S. Sheikhi-Mohammareh, A. Shiri, J. Mague, Dimroth rearrangement-based synthesis of novel derivatives of [1, 3] selenazolo [5, 4-e][1, 2, 4] triazolo [1, 5-c] pyrimidine as a new class of selenium-containing heterocyclic architecture, Mol. Divers. 26 (2022) 923–937.
[44] S. Bigonah-Rasti, S. Sheikhi-Mohammareh, K. Saadat, A. Shiri, Novel tricyclic 2-Alkoxy-8-methyl-6-(pyrrolidin-1-yl)-4 H -[1,2,4]triazolo[5,1- f]purine derivatives: synthesis and characterization, Polycycl. Aromat. Comp. (2020) 1–11, https://doi.org/10.1080/10406638.2020.1852287.
[45] A. Boultif, D. Louër, Indexing of powder diffraction patterns for low-symmetry lattices by the successive dichotomy method, J. Appl. Crystallogr. 24 (1991) 987–993.
[46] H.M. Rietveld, A profile refinement method for nuclear and magnetic structures, J. Appl. Crystallogr. 2 (1969) 65–71.
[47] R.A. Young, The Rietveld Method, International union of crystallography, 1993.
[48] J. Rodriguez-Carvajal, FULLPROF: a program for Rietveld refinement and pattern matching analysis, in: Satell. Meet. Powder Diffr. XV Congr. IUCr, 1990. Toulouse, France:[sn].
[49] H. Kobayashi, M. Ogawa, R. Alford, P.L. Choyke, Y. Urano, New strategies for fluorescent probe design in medical diagnostic imaging, Chem. Rev. 110 (2010) 2620–2640.
[50] K. Singh, A.M. Rotaru, A.A. Beharry, Fluorescent chemosensors as future tools for cancer biology, ACS Chem. Biol. 13 (2018) 1785–1798.
[51] M. Collot, T.K. Fam, P. Ashokkumar, O. Faklaris, T. Galli, L. Danglot, A. S. Klymchenko, Ultrabright and fluorogenic probes for multicolor imaging and tracking of lipid droplets in cells and tissues, J. Am. Chem. Soc. 140 (2018) 5401–5411.
[52] H.-J. Chen, C.Y. Chew, E.-H. Chang, Y.-W. Tu, L.-Y. Wei, B.-H. Wu, C.-H. Chen, Y.-T. Yang, S.-C. Huang, J.-K. Chen, S-cis diene conformation: a new bathochromic shift strategy for near-infrared fluorescence switchable dye and the imaging applications, J. Am. Chem. Soc. 140 (2018) 5224–5234.
[53] J.-P. Goddard, J.-L. Reymond, Enzyme assays for high-throughput screening, Curr. Opin. Biotechnol. 15 (2004) 314–322.
[54] L. Yuan, W. Lin, K. Zheng, L. He, W. Huang, Far-red to near infrared analyte-responsive fluorescent probes based on organic fluorophore platforms for fluorescence imaging, Chem. Soc. Rev. 42 (2013) 622–661.
[55] A. Mishra, R.K. Behera, P.K. Behera, B.K. Mishra, G.B. Behera, Cyanines during the 1990s: a review, Chem. Rev. 100 (2000) 1973–2012.
[56] X. Chen, T. Pradhan, F. Wang, J.S. Kim, J. Yoon, Fluorescent chemosensors based on spiroring-opening of xanthenes and related derivatives, Chem. Rev. 112 (2012) 1910–1956.
[57] Y. Gan, G. Yin, T. Yu, Y. Zhang, H. Li, P. Yin, A novel fluorescent probe for selective imaging of cellular cysteine with large Stokes shift and high quantum yield, Talanta 210 (2020), 120612.
[58] C. Würth, M. Grabolle, J. Pauli, M. Spieles, U. Resch-Genger, Relative and absolute determination of fluorescence quantum yields of transparent samples, Nat. Protoc. 8 (2013) 1535–1550.
[59] L. de O. Aguiar, E. Regis, P. Tuzimoto, E. Girotto, I.H. Bechtold, H. Gallardo, A. A. Vieira, Investigation of thermal and luminescent properties in 4, 7-diphenylethynyl-2, 1, 3-benzothiadiazole systems, Liq. Cryst. 45 (2018) 49–58.
[60] L. de O. Aguiar, A.S.L. Junior, I.H. Bechtold, S.F. Curcio, T. Cazati, T. V Alves, A. A. Vieira, Molecular 5, 8-π-extended quinoxaline derivatives as chromophores for photoluminescence applications, J. Mol. Liq. 296 (2019), 111763.
[61] C. Moon, K. Suzuki, K. Shizu, C. Adachi, H. Kaji, J. Kim, Combined inter-and intramolecular charge-transfer processes for highly efficient fluorescent organic light-emitting diodes with reduced triplet exciton quenching, Adv. Mater. 29 (2017), 1606448.
[62] A. Marini, A. Munoz-Losa, A. Biancardi, B. Mennucci, What is solvatochromism? J. Phys. Chem. B 114 (2010) 17128–17135.
[63] C. Reichardt, Solvatochromic dyes as solvent polarity indicators, Chem. Rev. 94 (1994) 2319–2358.
[64] M. Missioui, S. Mortada, W. Guerrab, G. Serdaroğlu, S. Kaya, J.T. Mague, E. M. Essassi, M.E.A. Faouzi, Y. Ramli, Novel antioxidant quinoxaline derivative: synthesis, crystal structure, theoretical studies, antidiabetic activity and molecular docking study, J. Mol. Struct. 1239 (2021), 130484.
[65] M. Zhang, Z.-C. Dai, S.-S. Qian, J.-Y. Liu, Y. Xiao, A.-M. Lu, H.-L. Zhu, J.-X. Wang, Y.-H. Ye, Design, synthesis, antifungal, and antioxidant activities of (E)-6-((2-phenylhydrazono) methyl) quinoxaline derivatives, J. Agric. Food Chem. 62 (2014) 9637–9643.
[66] H. Beyzaei, M.K. Deljoo, R. Aryan, B. Ghasemi, M.M. Zahedi, M. Moghaddam-Manesh, Green multicomponent synthesis, antimicrobial and antioxidant evaluation of novel 5-amino-isoxazole-4-carbonitriles, Chem. Cent. J. 12 (2018) 1–8.
[67] V. Sindhi, V. Gupta, K. Sharma, S. Bhatnagar, R. Kumari, N. Dhaka, Potential applications of antioxidants–A review, J. Pharm. Res. 7 (2013) 828–835.
[68] S. Li, S. Yuan, Q. Zhao, B. Wang, X. Wang, K. Li, Quercetin enhances chemotherapeutic effect of doxorubicin against human breast cancer cells while reducing toxic side effects of it, Biomed. Pharmacother. 100 (2018) 441–447.
[69] J. Xu, W.W. Du, N. Wu, F. Li, X. Li, Y. Xie, S. Wang, B.B. Yang, The circular RNA circNlgnmediates doxorubicin-inducedcardiac remodeling and fibrosis, Mol. Ther. Acids. 28 (2022) 175–189.
[70] H. Zhang, D. Sheng, Z. Han, L. Zhang, G. Sun, X. Yang, X. Wang, L. Wei, Y. Lu, X. Hou, Doxorubicin-liposome combined with clodronate-liposome inhibits hepatocellular carcinoma through the depletion of macrophages and tumor cells, Int. J. Pharm. 629 (2022), 122346.
[71] E. Pishavar, F. Oroojalian, M. Ramezani, M. Hashemi, Cholesterol-conjugated PEGylated PAMAM as an efficient nanocarrier for plasmid encoding interleukin-12 immunogene delivery toward colon cancer cells, Biotechnol. Prog. (2019), https://doi.org/10.1002/btpr.2952.

[72] M. Rahimizadeh, H. Eshghi, A. Shiri, Z. Ghadamyari, M.M. Matin, F. Oroojalian, P. Pordeli, Fe (HSO 4) 3 as an efficient catalyst for diazotization and diazo coupling reactions, J. Kor. Chem. Soc. 56 (2012) 716–719.
[73] F. Oroojalian, A.H. Rezayan, F. Mehrnejad, A.H. Nia, W.T. Shier, K. Abnous, M. Ramezani, Efficient megalin targeted delivery to renal proximal tubular cells mediated by modified-polymyxin B-polyethylenimine based nano-gene-carriers, Mater. Sci. Eng. C 79 (2017) 770–782.
[74] M.A. Karimi, M. Dadmehr, M. Hosseini, B. Korouzhdehi, F. Oroojalian, Sensitive detection of methylated DNA and methyltransferase activity based on the lighting up of FAM-labeled DNA quenched fluorescence by gold nanoparticles, RSC Adv. 9 (2019) 12063–12069.